Lab on a Chip

PAPER

View Article Online
View Journal | View Issue

Cite this: *Lab Chip*, 2019, **19**, 3268

Fish-gut-on-chip: development of a microfluidic bioreactor to study the role of the fish intestine *in vitro*†

Carolin Drieschner,[ab] Sarah Könemann,[ac] Philippe Renaud[b] and Kristin Schirmer *[acd]

In this study we present the first fish-gut-on-chip model. This model is based on the reconstruction of the intestinal barrier by culturing two intestinal cell lines from rainbow trout, namely epithelial RTgutGC and fibroblastic RTgutF, in an artificial microenvironment. For a realistic mimicry of the interface between the intestinal lumen and the interior of the organism we i) developed ultrathin and highly porous silicon nitride membranes that serve as basement membrane analogues and provide a culture interface for the fish cells; ii) constructed a unique micro-well plate-based microfluidic bioreactor that enables parallelization of experiments and creates realistic fluid flow exposure scenarios for the cells; iii) integrated electrodes in the reactor for non-invasive impedance sensing of cellular well-being. In a first approach, we used this reactor to investigate the response of epithelial fish cells to *in vivo*-like shear stress rates of 0.002–0.06 dyne per cm^2, resulting from fluid flow within the intestinal lumen. Moreover, we investigated the interplay of epithelial and fibroblast cells under optimal flow conditions to carefully evaluate the benefits and drawbacks of the more complex reconstruction of the intestinal architecture. With our fish-gut-on-chip model we open up new strategies for a better understanding of basic fish physiology, for the refinement of fish feed in aquaculture and for predicting chemical uptake and bioaccumulation in fish for environmental risk assessment. The basic principles of our reactor prototype, including the use of ultrathin membranes, an open microfluidic circuit for perfusion and the micro-well plate-based format for simplified handling and avoidance of air-bubbles, will as well be of great value for other barrier-on-chip models.

Received 30th April 2019,
Accepted 17th July 2019

DOI: 10.1039/c9lc00415g

rsc.li/loc

Introduction

Fish intestinal epithelia are important gatekeepers and communicators between fish and the surrounding environment. They regulate the interaction with fresh- or saltwater milieus, food, microorganisms and xenobiotics.[1] As fish are early indicators for aquatic ecosystem health,[2] understanding compromised intestinal barrier function has significant implications for the field of environmental toxicology and aquaculture industry.[3]

Our current knowledge of the fish intestine largely originates from *in vivo* experiments[4] or *ex vivo* gut sac preparations to study *e.g.* intestinal absorption of iron as essential metal.[5] However, difficult accessibility and the trend towards ethically justifiable, low cost and simplified *in vitro* systems[6] call for the development of fish cell line-based intestinal barrier models.

The RTgutGC cell line, derived from the epithelium of the intestine of rainbow trout,[7] has previously been implemented in commercial trans-well inserts, allowing to study the physiological and toxicological response of the cells *e.g.* during simulated seawater adaptation and silver exposure,[8] as well as intestinal uptake of potential hazardous nanomaterial[9] and hydrophobic chemicals.[10]

Yet, commercial inserts have limitations, such as low permeability of the polymeric cell culture membrane and limited visibility of cells.[11,12] These limitations have led to the development of ultrathin nanoporous alumina membranes,[13] which allowed the establishment of an intestinal co-culture model of epithelial RTgutGC and newly developed fibroblastic RTgutF cell lines to partially reconstruct the complexity of the intestinal wall for improved barrier functionality.[14] However, culture conditions are stagnant which is not reflective of the *in vivo* situation.

[a] *Department of Environmental Toxicology, Eawag (Swiss Federal Institute of Aquatic Science and Technology), Dübendorf, Switzerland.*
E-mail: kristin.schirmer@eawag.ch
[b] *Microsystems Laboratory 4, School of Architecture, EPFL (École Polytechnique Fédérale de Lausanne), Lausanne, Switzerland*
[c] *Department of Civil and Environmental Engineering, School of Architecture, EPFL (École Polytechnique Fédérale de Lausanne), Lausanne, Switzerland*
[d] *Department of Environmental Systems Science, ETHZ (Swiss Federal Institute of Technology in Zurich), Zürich, Switzerland*
† Electronic supplementary information (ESI) available. See DOI: 10.1039/c9lc00415g

The current development of microfluidic cell culture devices to mimic the human intestine (human-gut-on-chip) enables the culture of cells under physiological realistic conditions by exposing them to fluid flow. Herein, epithelial cells (Caco-2) are typically cultured on a microporous, several micrometer thick membrane and perfused through a closed microfluidic circuit. Trans-epithelial electrical resistance (TEER), a measure of epithelial tightness, is usually quantified by placing chopstick or wire electrodes into the microfluidic channels.[15–17]

In our study, we report on the development of the first prototype fish-gut-on-chip device that provides *in vivo*-like culture conditions for rainbow trout intestinal cells. The open-microfluidic platform combines established culture ware with an engineered microsystem to enable facilitated handling on the one hand and a controllable microenvironment for cells on the other. Our study explored the potential of ultrathin silicon nitride membranes for epithelial-barrier-remodeling under flow conditions. The response of piscine intestinal epithelial cells alone or in combination with fibroblasts to shear stress was monitored by reactor integrated platinum electrodes for TEER evaluation and by fluorescence microscopy. Overall, the fish-gut-on-chip platform incorporates several innovations compared to previously described gut-on-chip designs and provides a novel system for investigating the role and function of the fish intestine.

Material and methods

Reactor design and fabrication

The fish-gut-on-chip device consists of a number of different components. Their fabrication and integration is described in this section. The final design is presented in the results.

Silicon nitride (SiN) porous supports. SiN porous supports were manufactured for microfluidic applications and are the centrepiece of the fish-gut-on-chip device. In the following they will be termed SiN_{FLOW} chips. SiN_{FLOW} chips were fabricated by applying the procedure outlined by Kuiper *et al.* (1998).[18] Briefly, a 500 nm thick layer of low stress SiN was thermally grown by low pressure chemical vapour deposition on both sides of standard (∅ 100 mm, 380 μm thick, <100> oriented, double side polished) silicon wafers. Standard photolithography and reactive ion etching were used to pattern SiN films on both sides of the wafer. The pattern on the bottom side defined the pore size (∅ 1.2 μm) and pore arrangement on the permeable membrane. The structures on the top side specified the chip size by formation of cleavage lines and openings to form an etch mask for the membrane formation process. In a subsequent step, anisotropic chemical etching in potassium hydroxide (KOH) solution was used to release free-standing SiN membranes from silicon. Individual chips (24 per wafer, dimensions: 22.5 mm × 9 mm) were obtained by manual cleavage along the cleavage lines. Each chip contains two parallel rectangular cavities that culminate into the porous SiN membrane (10 mm × 1 mm) and serve as future upper microfluidic channels with a pyramidal geometry that resulted from KOH etching. A square opening, culminating into a non-porous SiN membrane (1 mm × 1 mm), is located at each end of the channels. The non-porous SiN membranes were removed with scotch tape, thus the openings clear the path for microfluidic connection to the bottom side of the chip. Membrane images were taken using a Zeiss LEO 1550 scanning electron microscope.

Polydimethylsiloxane (PDMS) sheets. PDMS sheets were attached on both sides of SiN_{FLOW} chips to confine microfluidic channels. The sheets were fabricated by spin coating of PDMS. Therefore, PDMS-based agent and curing agent (Sylgard 184, Sigma Aldrich, Switzerland) were mixed in a 10 : 1 weight ratio. After degassing, this mixture was spin coated onto a silanized silicon wafer (∅ 100 mm, single side polished) at 100 rpm for 60 s. Silanization was performed by evaporation of chlorotrimethylsilane (TMCS, Sigma Aldrich, Switzerland) to form a passivation layer on the wafer surface that allows simple PDMS detachment. Subsequently, PDMS was cured for at least 2 h at 80 °C. A thickness of 1 mm of the PDMS layer was determined with a digital measuring slide. The PDMS sheets were cut to shape by using a pre-manufactured aluminium template, a scalpel and a puncher (ESI,† Fig. S1). The top PDMS sheet is characterized by 10 holes: 4 for inlets, 4 for outlets and 2 for electrode access. This sheet was used to define the upper microfluidic channel, which is integrated in the SiN_{FLOW} chip (dimensions: height: 0.38 mm, base area: 10 × 1 mm, wall angle from pyramidal KOH etching: 35.26°, volume: 5 μL). The bottom PDMS sheet contains two rectangular openings to serve as lower microfluidic channels (dimensions: height: 1 mm, width: 1.5 mm, length: 20 mm, volume: 30 μL).

Basic platform. A modified micro-well plate was used as platform for reactor assembly on the plates bottom and perfusion from top micro-wells. A 384-well polystyrene microplate and associated lid (Greiner Bio-One, Switzerland) were adapted by hole drilling for microfluidic and electrode connections and for sampling of microchannel eluates. Milling of micro-well walls, to connect individual wells, was performed to create a down-grade slope from in- to outlets to allow for an open microfluidic circuit and to generate a drainage. In detail, outlet well and adjacent drainage well were connected *via* partial milling (6 mm) of the well wall and drainage wells were interconnected by total milling (9 mm) of connecting well walls. The drain was integrated in the side wall of the microplate by hole-drilling and gluing of a shortened flow connector (∅ 8 mm, NORMAPLAST, Tecalto, Switzerland) with two-component epoxy adhesive (Loctite M-21HP Hysol, Henkel). A tubing (∅ 7.5 mm, silicone, Fisher Scientific, Switzerland) was fixed to the drain connector on one side and to a collection reservoir (50 mL Falcon tube, TPP, Switzerland) on the other. For open microfluidics, tubings (PTFE, inner ∅: 1.06 mm; Fischer Scientific, Switzerland) were fixed into appropriate holes within the lid using short pieces of flexible tygon tubing (Sigma Aldrich, Switzerland) as adapters. For perfusion, the micro-well plate was closed with the lid and tubings were connected to medium filled syringes

(Once/Codan, Huber, Switzerland), which were installed on a microfluidic pump (NE-1000, SyringePump, Switzerland).

Electrodes. Electrodes for impedance sensing were integrated in the fish-gut-on-chip device. The top electrode was created by implementing a platinum (Pt) wire ∅ 0.3 mm (Advent Research Material, England) in the centre of the upper microfluidic channel *via* a hole in the bottom of the microwell plate. The wire was glued (adhesive silicone CAF3, Bluestar Silicones, Silitech, Switzerland) into the appropriate well of the microplate to avoid leakage and wire dislocation during measurements. The bottom electrode was manufactured using standard photolithography lift-off technique to obtain a planar Pt electrode (1 mm × 8 mm) on glass substrate. Electrodes composed of a 20 nm thick titanium adhesion layer and a 200 nm thick Pt layer were sequentially evaporated on a float glass wafer (∅ 100 mm, 525 μm thick) (LAB 600H evaporator, Leybold Optics). Individual electrode platelets (18 mm × 22 mm) were obtained by dicing of the wafer. The active electrode sensing area (1.5 mm^2) was determined by attaching the glass platelet to the bottom PDMS sheet, which forms the lower microfluidic channel. Electrode connection for impedance sensing was realized with spring contacts (3 A 24.64 mm round head and 90° concave, Distrelec, Switzerland) mounted from the top of the microwell plate.

Polycarbonate (PC) platelets. The installation of the PC platelets was done to avoid leakage and to strengthen the assembly of the whole composition. PC platelets (3.4 mm × 4.9 mm × 2 mm) were obtained by trimming of PC plates (Röhm, Switzerland) and hole-drilling for screw connection.

Sterilization and reactor assembly. Prior to reactor assembly, PDMS sheets were cleaned from dust using Scotch tape and all reactor parts were sterilized with ethanol (70%) for 10 min, dried under a sterile bench, and exposed to UV light for 30 min. Microfluidic tubings and syringe connectors (Rotilabo, Roth, Switzerland) were autoclaved. For reactor assembly, all parts were aligned to the modified bottom of the microplate in the following order: upper PDMS sheet – SiN_{FLOW} chip – lower PDMS sheet – electrode platelet – PC platelets. Individual parts, besides PC platelet, stuck together by the adhesive nature of PDMS.

Cell culture

Cell lines and culture conditions. Experiments were performed with the epithelial cell line RTgutGC[7] and the fibroblast cell line RTgutF,[14] both established from the intestine of rainbow trout. Cells were routinely grown in Leibovitz's L-15 medium (Invitrogen, Switzerland), supplemented with 5% fetal bovine serum (FBS; PAA, Switzerland) for RTgutGC and 10% FBS for RTgutF, and 1% gentamycin (GIBCO, Invitrogen, Switzerland). Cells were maintained at 19 ± 1 °C under normal atmosphere in the dark.

Preparation of fish-gut-on-chip device. Prior to cell seeding in the fish-gut-on-chip device, microfluidic channels were filled with ethanol (70%), incubated for 5 min and replaced stepwise by sterile MilliQ water to avoid the formation of air bubbles. Then, the upper channel was flushed thrice with 100 μL of coating solution, containing 50 μg μL^{-1} fibronectin in sterile water and incubated for 4 h. Thereafter, coating solution in the channel was replaced by L-15/FBS (5%). For the co-culture setting, the lower channel was coated subsequently with the same procedure, but during coating the in- and outlet wells were closed with a sterile sealing foil (Fisher Scientific, Switzerland) and the whole fish-gut-on-chip assembly was placed upside down. It is important that solutions are never removed from microfluidic channels but that liquids are gently replaced by adding the new solution through inlet wells, which results in flushing of the channels.

Cell seeding. Cell seeding of monocultures of RTgutGC was obtained by flushing the upper channel with 2 × 100 μL of cell suspension containing 1.4 × 10^6 cell per mL in L-15/FBS (5%). After cell attachment, occurring within 30 min, the upper channel was flushed thrice with 100 μL of L-15/FBS (5%) to remove unattached cells. For co-culture establishment, RTgutF cells were seeded first in the lower channel by filling the channel with cell suspension containing 55 000 cell per mL in L-15/FBS (10%), closing the in- and outlet wells with foil, and placing the reactor upside down to allow cell settling on the membrane. After 30 min, the reactor was turned back, the lower channel flushed thrice with 100 μL of L-15/FBS (10%) and RTgutGC cells were seeded as described above. After the mono- or co-culture seeding procedure, cells were incubated at 19 ± 1 °C under normal atmosphere in the dark for two days prior to flow application.

Flow application. For flow application, the upper channel was perfused at various flow rates (20 μL h^{-1}, 200 μL h^{-1}, 600 μL h^{-1}), resulting in very low to moderate shear stress of, respectively, 0.002 dyne per cm^2, 0.02 dyne per cm^2 and 0.06 dyne per cm^2, on the apical surface of RTgutGC cells. Perfusion of the lower channel (200 μL h^{-1}) ensured fresh media supply from the basolateral side of RTgutGC cells and, if present, sustained cell viability of RTgutF cells, while creating only minimal shear stress (0.002 dyne per cm^2). Of note, the difference in resulting shear stress in the upper and lower channel result from their different geometries (see "Polydimethylsiloxane (PDMS) sheets"). Shear stress (τ, dyne per cm^2) was calculated according to the following equation:

$$\tau = \frac{6\mu Q}{h^2 w}$$

Herein, μ is the viscosity of the culture medium (g cm^{-1} s), Q is the volumetric flow rate (cm^3 s^{-1}), h is the channel height (cm) and w is the channel width (cm). For static cultures, serving as control, channels were flushed with new medium (2 × 100 μL) on a daily base.

Epithelial barrier measurements

Impedance spectroscopy was performed to determine transepithelial electrical resistance (TEER), a common marker for

tight junction integrity,[19] of RTguGC monolayer and co-cultures with RTgutF. Baseline resistance (membrane without cells) was obtained prior to cell seeding and subtracted from the resistance generated by cells cultured on the membrane prior to calculation of TEER (in Ω cm^2). Impedance spectra were recorded from 100 Hz–5 MHz at an amplitude of 20 mV using an impedance analyser (MFIA, Zurich Instruments, Switzerland).

Triton exposure

A proof-of-principal experiment for detecting changes in impedance due to chemical stress was performed on two days old RTgutGC cultures, which were kept under static conditions in the fish-gut-on-chip device. To accomplish this, cells were exposed to different concentrations of Triton X-100 (Sigma Aldrich, Switzerland) in L-15/FBS (5%) ranging from 0.125–0.2%.

Characterization of cellular features

Phase-contrast imaging. Images of cells cultured on SiN membranes were taken with Leica DMI600 inverted microscope.

Immunocytochemistry. Immunocytochemical staining of plasma membrane (cell mask) and cell nuclei (DAPI stain) of live cells was applied to determine cell density and cell height after exposure to various shear stress conditions. Cellular polarization was analyzed by staining of the tight junction protein ZO-1, cytoskeletal f-actin (phalloidin) and cell nuclei (DAPI stain) on fixed cells. Prior to staining, SiN_{FLOW} chips accommodating cultured cells on SiN membranes were disassembled from the microfluidic reactor.

For live staining, cells were washed thrice in phosphate buffered saline (PBS) and cell mask deep red plasma membrane stain (7.5 μg mL^{-1} in PBS, Thermo Fisher, Switzerland) was applied together with DAPI stain for 8 min at room temperature. Subsequently, cells were washed thrice in PBS and SiN_{FLOW} chips were mounted onto microscope slides.

Fixed staining of ZO-1, f-actin and DAPI followed the same procedure as described previously.[13] Briefly, cells were fixed in 3.7% paraformaldehyde (Invitrogen, Switzerland) in PBS for 10 min, followed by a quick washing step and permeabilization with 0.2% Triton X-100 in PBS for 15 min. After a further washing step with PBS, containing 0.1% Triton X-100, cells were incubated in Image-iT (Invitrogen, Switzerland) for 30 min and washed with PBS. Then, primary antibody for tight junction staining (5 μg mL^{-1}, Alexa Fluor-coupled ZO-1 antibody, Invitrogen, Switzerland) was applied together with FITC coupled phalloidin (1 : 100; Sigma-Aldrich, Switzerland) in 0.5% goat serum and 0.05% Triton X-100 in PBS overnight at 4 °C. The next day, cells were washed with 0.1% Triton X-100 in PBS and subsequently incubated with 10.9 μM DAPI (Invitrogen, Switzerland) in PBS for 5 min. After repeated washing in 0.1% Triton X-100 in PBS and PBS only, SiN_{FLOW} chips were mounted on microscope slides using ProLong Gold antifade reagent (Life Technology, United States).

Imaging and analysis were performed on a Leica SP5 laser scanning confocal microscope (Leica, Switzerland) using the LAS AF Lite 2014 software.

Statistical analysis

Results were represented as mean ± standard deviation (SD) with n indicating the number of independent conducted experiments. Statistical analysis was performed using Graphpad Prism® software (Prism 7.04 for Windows) by performing two-way ANOVA, together with Tukey's *post hoc* test (Fig. 3A). The level of significance was set at probabilities of $^*p < 0.05$, $^{**}p < 0.01$, $^{***}p < 0.001$ and $^{****}p < 0.0001$.

Results and discussion

Design and characterization of the fish-gut-on-chip model

The fish-gut-on-chip device was designed to recapitulate the microenvironment of the piscine intestine by mimicking flow phenomena within the lumen and rapid crosstalk between absorptive epithelial cells lining the intestinal wall and supportive fibroblasts present in the underlying connective tissue. The device has the typical "epithelium-on-chip" geometry, which consists of two parallel microfluidic channels separated by a permeable membrane.

In contrast to many microfluidic barrier models, which use non-physiological, several micron thick permeable membranes as support for cell growth,[15–17,20] we developed the fish-gut-on-chip device by integrating an ultrathin, highly permeable SiN membrane (Fig. 1). The membranes are framed in silicon chips and fabricated as array on silicon wafers. Individual chips are termed SiN_{Flow} chip and comprise two experimental units for separate handling, where each unit incorporates a rectangular SiN membrane for cell culture and

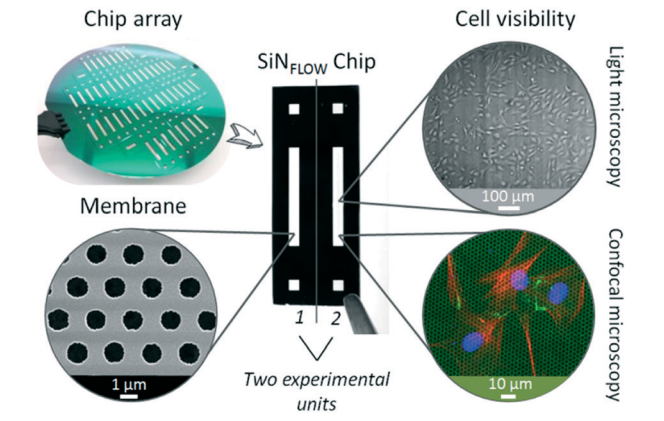

Fig. 1 Silicon nitride porous supports. Silicon nitride (SiN) membranes are fabricated within individual chips (SiN_{Flow} chip) in silicon wafers. Each chip is composed of two experimental units. Membranes are characterized by high porosity (scanning electron microscopy image, bottom left), transparency for cell monitoring (light microscopy, top right) and a thickness of only 500 nm that allows fluorescence microscopy of cells through the membrane (bottom right, membrane in green from laser reflection, cells are stained for cell nucleus in blue, cytoskeleton in red and tight junction protein ZO-1 in green).

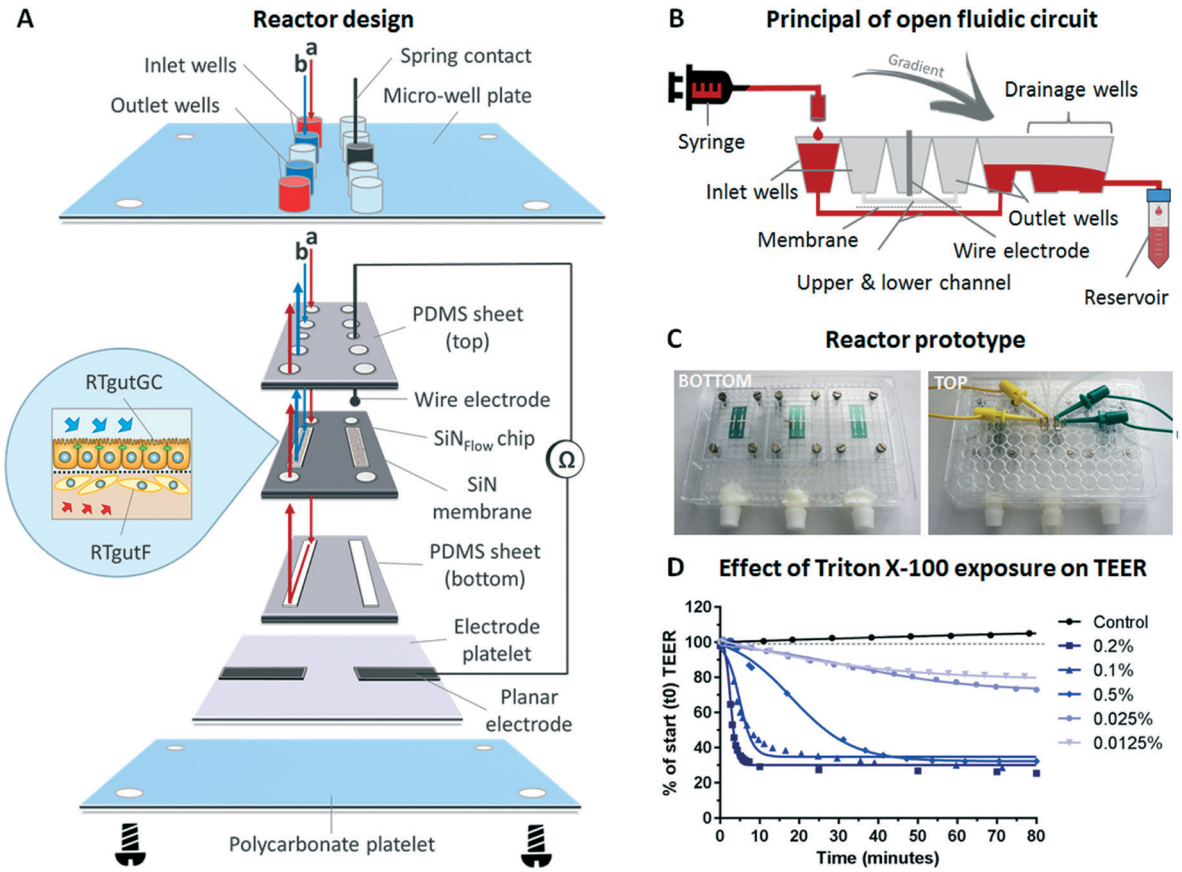

Fig. 2 The fish-gut-on-chip model. (A) The device is composed of a modular stacked assembly of the SiN_{Flow} chip sandwiched between two sheets of PDMS and an electrode platelet from the bottom. This arrangement is screwed to the bottom of a modified 384 micro-well plate using a polycarbonate platelet. The micro-well plate format allows for simplified perfusion of the upper and lower microfluidic channels from the top micro-wells and connection to reactor integrated electrodes with spring contacts. Membrane magnification depicts conceptual cell culture of epithelial RTgutGC and fibroblastic RTgutF cells on opposite membrane sides. (B) Working principal of open microfluidic circuit sketched for the lower microfluidic channel on a partial cross-section of the micro-well plate. (C) Photographs of bottom and top side of the reactor. Bottom view: 3 SiN_{Flow} chips are assembled on the well plate. Top view: The middle chip is connected with tubing's for perfusion and cables for impedance spectroscopy. (D) Effect of varying concentrations of Triton X-100 on barrier tightness of the RTgutGC monolayer.

two square openings for perfusion of the bottom channel. The SiN membranes feature a thickness of only 500 nm, a pore size of ~1.2 μm diameter and a porosity of 24%. This makes SiN membranes more comparable to the highly permeable basement membrane, which is found *in vivo* between different biological compartments, such as epithelium and underlying connective tissue in the intestine.[21] Moreover, SiN membranes are optically transparent and allow perfect visibility of cells during phase contrast imaging and fluorescence microscopy, even when imaging is performed through the membrane. Previous studies demonstrated the utility of thin SiN porous supports for nanoparticle translocation studies on static *in vitro* models of the human blood–brain-barrier[22] and human alveolar barrier,[12] which is problematic with conventional permeable cell culture membranes due to their thickness (≥10 μm).[11,12] Indeed, the production of SiN membranes, requiring clean room fabrication processes, is more expensive than production of conventional polymeric culture membranes composed of *e.g.* polyethylene terephthalate (PET) or polycarbonate (PC). However, SiN porous supports are very robust and can be reused several times by applying the cleaning method outlined by Kenzaoui *et al.* (2013).[22]

Cell culture and flow application on the newly developed SiN_{Flow} chips is achieved by integration of the chip within the fish-gut-on-chip device. The device combines several novelties; an overview of its assembly and working principal are depicted in Fig. 2. Conceptually, the fish-gut-on-chip system is assembled on the bottom of a modified micro-well plate to allow for simplified reactor handling through the micro-wells from the top, which includes coating, cell seeding, microfluidic and electrode connection and sampling of microchannel outflow (Fig. 2A). Microfluidic channels are defined by sandwiching the SiN_{FLOW} chip between two sheets of patterned PDMS. From the bottom side the assembly is closed by a glass platelet with integrated planar electrodes for TEER evaluation and a polycarbonate platelet for fixation to the micro-well plate. The thickness of the modular stack on the bottom of the micro-well plate is less than 5 mm in total and allows for microscopic investigation of cells cultured on the SiN membrane from the bottom. For rearrangement of the

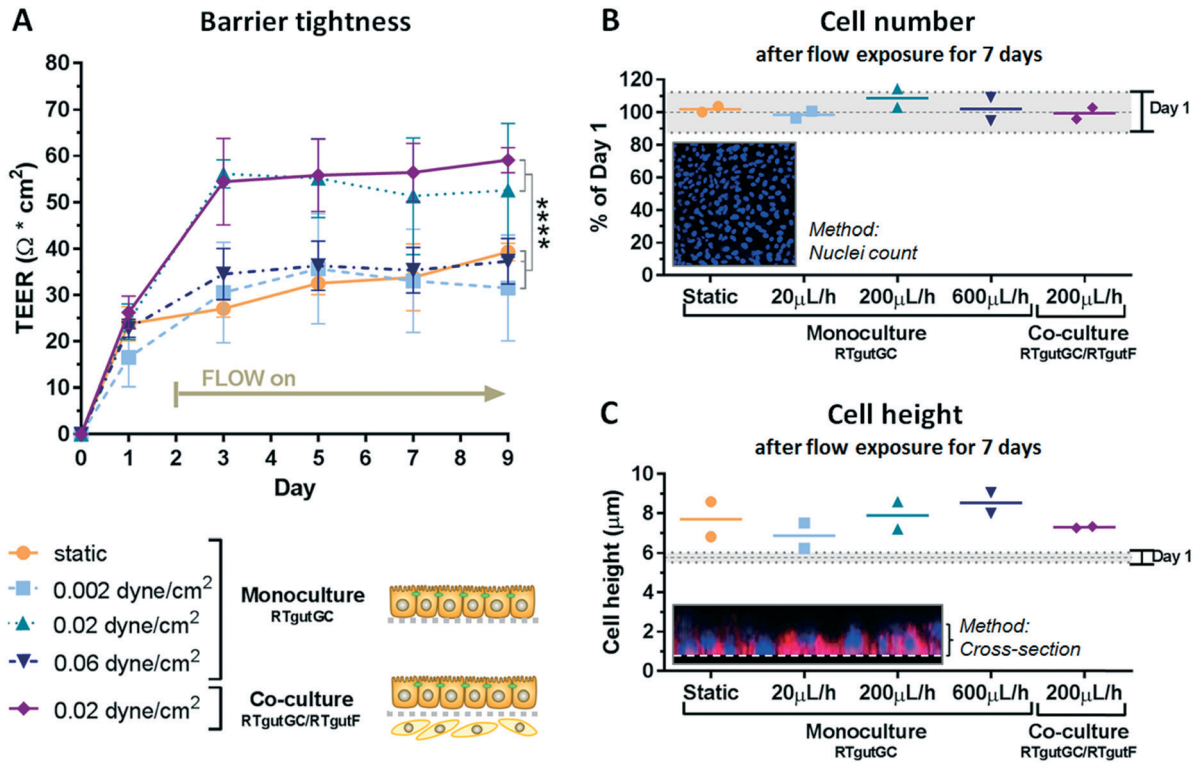

Fig. 3 Impact of shear stress on epithelial barrier organization. Effect of shear stress on the artificial fish gut was evaluated with TEER analysis (A), proliferation assessment (B) and cell height determination (C). RTgutGC cells were exposed to different flow rates on the apical surface, which resulted in shear stress of 0.002–0.06 dyne per cm^2. TEER data represent the mean ± SD; $n \geq 3$. The statistical differences are denoted: $p < 0.0001$ by ****. For cell number and cell height, 2 biological replicates and their mean are represented.

piscine intestinal mucosal architecture, epithelial RTgutGC and fibroblastic RTgutF cells can be cultured on opposite membrane sides. This allows to create asymmetric exposure conditions: one channel simulates realistic flow rates and a medium composition as found in the intestinal lumen; and the other mimics the steady renewal of nutrients from the blood circulation.

For flow application, an open microfluidic circuit was implemented in the fish-gut-on-chip device (Fig. 2B). Herein, perfusion of microfluidic channels is enabled by closing the micro-well plate-based reactor with a modified lid, which is equipped with tubings that connect to the respective syringes. The drop-wise filling of the inlet wells from syringe-connected tubings results in perfusion of the upper and/or lower channel. Subsequently, the outlet wells are filled with liquid, which flows over to the drainage wells due to gradient driven forces along the down-grade slope of interconnected micro-wells. The outflow is finally collected in an installed reservoir. This perfusion strategy simplifies connection and disconnection of microfluidic tubings and prevents air bubble formation in the microfluidic channels, which is a serious obstacle for long-term cell-culture in microfluidic systems.[23,24] Open microfluidics can be applied for low- to midrange flow rates, as required to simulate fluid flow in the intestine.[15] Very high flow rates, as applied for *in vitro* blood vessel models,[25] might not be possible because the pressure to force fluids through the microfluidic channels is limited.

For parallelization of experiments, which is a major goal for facilitated organ-on-chip application,[26] each microplate was equipped with three SiN_{FLOW} chips, with each being composed of two experimental units (Fig. 2C). Thus, a total of six experimental conditions can be tested simultaneously. Connection to microfluidic tubings and electrodes for impedance-based TEER measurements were established through the micro-well plate lid (Fig. 2C), which can be removed during experimentation. This facilitates manipulation of individual chips, *e.g.* for microscopy of samples at different time points.

The functional formation of an epithelial barrier by RTgutGC cells within the fish-gut-on-chip device was verified with TEER measurements. Impairment of the cellular barrier through exposure to different concentrations of Triton X-100, a non-ionic surfactant known to permeabilize the cell membrane,[27] was performed as proof-of-principal to test the reliability of measurements obtained through reactor integrated platinum electrodes (Fig. 2D). During Triton X-100 exposure, RTgutGC cells showed a concentration dependent decline in TEER, expressed in percent of the resistance prior exposure. Effects for concentrations between 0.05–0.2% were observed immediately within the first min of exposure and resulted in a rapid decline of resistance within 5–40 min down to ~30%. The 30% threshold most likely represents the resistance of dead cells, which remained attached to the culture surface. Indeed, Triton X-100 concentrations of 0.1% and 0.2% are

used for cell membrane permeabilization within 15 min during immunocytochemical staining (see protocol in Materials and methods). The excessive membrane permeabilization at these concentrations results in cell death.[28] Lower concentrations of 0.0125 and 0.025% showed a steady but less steep decline to 70–80% within the exposure time of 80 min compared to control TEER values. TEER in this specific case reflects cell viability and the obtained values therefore are in the same range as previously reported EC_{50} values for 2 h exposure of fish and mammalian cells obtained from viability assays.[28] Hence, we demonstrated the successful application of on-line TEER evaluation by impedance spectroscopy in order to monitor barrier tightness of the RTgutGC epithelial cell layer. Further improvement of TEER recording might be obtained by the 4-point impedance measurement approach, which requires the integration of four electrodes, two on each side of the permeable membrane. This could be wire electrodes inserted in channel in- and outlets[29] or micro-fabricated, planar and preferentially semi-transparent electrodes on solid support[30] to still allow for visual inspection of cells. The 4-point technique makes TEER evaluation more robust by reducing variations of non-biological origin, *e.g.* from small changes in temperature or medium composition.[31]

Response of the gut-on-chip to shear stress

To explore the physiological relevance of mimicking shear stress, epithelial RTgutGC cells were grown at first as monocultures under different flow conditions, followed by initiation of co-culture with fibroblastic RTgutF cells at one selected flow rate. For experimentation, the upper channel was lined by RTgutGC intestinal epithelial cells and the perfusion with culture medium resulted in a shear stress of 0.002, 0.02 or 0.06 dyne per cm^2 respectively, after two days of pre-culture under static conditions. These shear rates have been selected to simulate the broad range of physiological flow occurring in the human intestine.[15] Perfusion of the lower channel mimicked the basolateral supply with nutrients from the blood stream. The applied constant flow caused very low shear stress of 0.002 dyne per cm^2 on intestinal RTgutF fibroblasts, if present. The response of the epithelial cells was compared to cells cultured under static conditions within the fish-gut-on-chip device and was evaluated by measuring TEER and by microscopic analysis of (i) cell density by nuclei staining and (ii) cell height by cell membrane staining (Fig. 3).

TEER analysis of RTgutGC monolayer revealed a significant increase from ~30 Ω cm^2 for static cultures and those exposed to low shear stress of 0.002 dyne per cm^2 to ~55 Ω cm^2 for cultures experiencing a moderate shear stress of 0.02 dyne per cm^2 already after day 3 and till day 9 of culture (Fig. 3A). Hence, RTgutGC cells seem to adapt to moderate shear stress by an increase in barrier tightness. Likewise, an increase in TEER upon the same shear stress (0.02 dyne per cm^2) compared to static cultures has been reported for human intestinal cells, where the authors suggested that mechanical distortion might alter the formation of tight junctions.[15] In contrast, TEER values obtained for RTgutGC monolayer exposed to high shear stress of 0.06 dyne per cm^2 were again comparable to values obtained for static and low shear stress (0.002 dyne per cm^2) conditions. Overall, the resistance values of RTgutGC monolayer cultured under static conditions in the microfluidic bioreactor are in accordance with previously reported values obtained in static cell culture inserts[8,9] and on ultrathin alumina membranes.[13] For freshwater adapted Atlantic salmon (*Salmo salar*), TEER values between 30 and 150 Ω cm^2 have been reported from isolated gut-sac preparations, which are composed of the epithelial cell layer and the underlying fibroblasts;[32] thus RTgutGC cell cultures under static and flow conditions generally closely reflect the *in vivo* TEER in salmonids. The reconstruction of the epithelial–mesenchymal interface by combining RTgutGC and RTgutF cells on opposite membrane sides under flow conditions resulted in stable TEER values of ~55–60 Ω cm^2 from day 3–9. Thus, the combination of flow and a supportive lamina of fibroblasts had no additional effect on TEER when compared to RTgutGC monolayer under flow conditions. In a previous study, where we combined RTgutGC and RTgutF cells under static conditions on ultrathin alumina membranes, we found an additive effect of TEER values of the two cell lines.[14] This effect seems to be less distinct in our flow-through system, suggesting that shear stress on the epithelial interface is the driving force for epithelial resistance modulation.

For cell seeding of RTgutGC we chose a density that allowed formation of a tightly packed monolayer. This leads to contact inhibition and cell cycle arrest in normal epithelial cells.[33] Indeed, RTgutGC cells showed no or very low proliferative activity when compared to day one of the static system (Fig. 3B). In addition, proliferation was not modulated by any of the treatments, which makes the system more robust during the test period. These results are consistent with previous studies demonstrating that RTgutGC remain in monolayer for at least 14 days when seeded at a similar density on permeable membranes.[8,13]

In the fish-gut-on-chip device, RTgutGC cells possessed a height of ~6 μm at day 1. During the culture period of 9 days, cells increased only marginally in height to 7–9 μm, which was independent of flow and co-culturing (Fig. 3C). The flattened morphology is a typical adaptation of static *in vitro* cell cultures, however, introduction of physiological stimuli, *i.e.* fluid flow, is considered to promote cellular re-adaptation to their original morphology.[34] In the fish intestine *in vivo*, enterocytes possess a columnar shape and a height of ~30 μm.[35] In the human-gut-on-chip model by Kim *et al.* (2012),[15] the mechanical stimulation of human intestinal epithelial (Caco-2) cells with fluid shear stress of 0.02 dyne per cm^2 was sufficient to increase cell height from 6 μm to 30 μm. The continued flattened morphology of RTgutGC cells during exposure to the same shear stress conditions might indicate a lower potential to differentiate into functional enterocytes, under the thus far explored conditions. Caco-2 cells, in contrast, were found to express strong tight

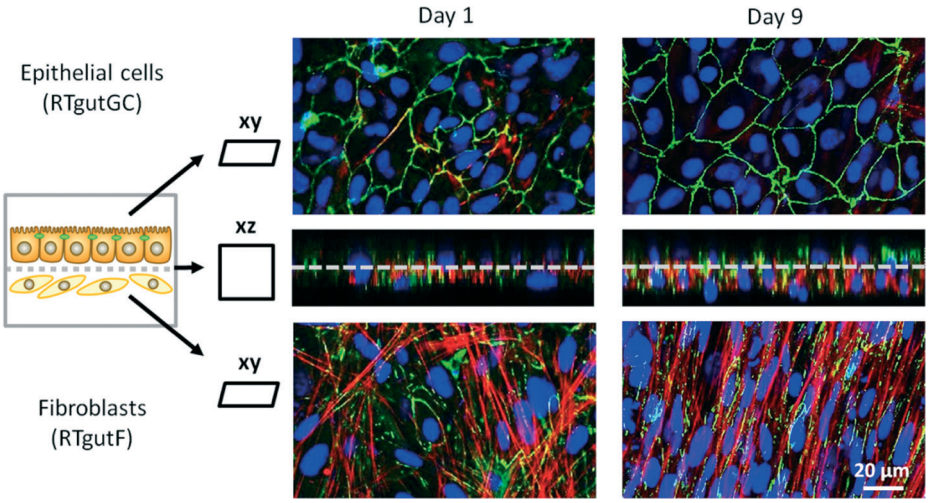

Fig. 4 Co-culture of piscine intestinal epithelial (RTgutGC) and fibroblast (RTgutF) cell lines. Cells were cultured for 9 days in the fish-gut-on-chip device, with RTgutGC being exposed to a shear stress of 0.02 dyne per cm^2 and RTgutF being exposed to 0.002 dyne per cm^2. Cells were stained for the tight junction protein ZO-1 (green), cytoskeletal f-actin (red) and nuclei (blue) and a complete *z*-stack from both sides was performed from top and through the membrane with confocal microscopy. The *xz* projection (middle images) show the close interaction between RTgutGC (TOP) and RTgutF (BOTTOM) grown on ultrathin porous SiN membranes. The *xy* projection revealed a dense and confluent monolayer of RTgutGC cells on day 1 and day 9. In contrary, RTgutF cells, established as monolayer (day 1), showed multilayer formation at day 9.

junctions and to form microvilli for apical surface enlargement, even when cultured under static conditions for an extended culture period of 21 days.[36]

The co-culture of epithelial RTgutGC and fibroblastic RTgutF cells is an advanced approach to better mimic the complexity of the intestinal wall.[14] Having established fluid flow now allowed to examine the expression of the tight junction protein ZO-1, orientation of cytoskeletal f-actin and general cellular organization under realistic shear flow conditions (0.02 dyne per cm^2 on RTgutGC cells) (Fig. 4). As demonstrated previously, RTgutGC cells express ZO-1 as continuous line on the apical cell boarder already at day 1 (ref. 8 and 13) and expression remains stable until day 9. In contrast, RTgutF cells exhibit only scattered ZO-1 patterns, which is coherent with the basic characterization of the RTgutF cell line[14] and the fact that fibroblasts do not form functional tight junctions.[37] Clear differences were found in actin skeleton organization in RTgutF over time under flow: while actin fibers formed an unorganized network at day 1, they were found to be aligned and tightly packed at day 9. Furthermore, RTgutGC cells remained in a monolayer over the culture period, whereas RTgutF cells, originally seeded as monolayer (day 1), proliferated and formed a multilayer of 2–3 levels (day 9) (Fig. 4, cross-section, DAPI stain).

The fact that the fibroblasts proliferate while the epithelial cells do not, adds a dynamic component that needs to be considered when doing time-resolved analyses. The established co-culture model is particularly valuable for understanding the role of the fish intestine as immunological barrier. Herein, fibroblasts present an immune competent cell type, which releases cytokines to attract other cell types of the intrinsic immune system *e.g.* upon stimulation through bacterial toxins.[37]

Conclusion

The fish-gut-on-chip device provides a controllable innovative microfluidic platform to study critical barrier functions in the presence of relevant physiological cues, including fluid flow and coexistence of supporting fibroblasts. Characterization of the model revealed that physiological, realistic fluid flow and shear stress, as experienced in the living intestine, is sufficient to promote stable intestinal epithelial tightening, which is enhanced compared to static piscine intestinal barrier models. The co-culture of epithelial cells and fibroblasts for reconstructing basic intestinal architecture is supported particularly through the ultrathin and porous SiN membrane, which serves as cell culture interface. The fish-gut-on-chip device may therefore facilitate studies of, *e.g.*, xenobiotic uptake or immunological defense mechanisms. Given the modularity of the device and the flexibility of its set-up, other epithelial barrier systems of fish or other organisms, including humans, might also be modelled with this device.

Conflicts of interest

There are no conflicts to declare.

Acknowledgements

This study was financially supported by Swiss National Science Foundation, Grant No. CR2312_144289.

References

1 M. Grosell, A. P. Farrell and C. J. Brauner, *The multifunctional gut of fish*, Elsevier, 2011.
2 J. H. Harris, *Austral Ecol.*, 1995, **20**, 65–80.

3 F. Jutfelt, *Encyclopedia of fish physiology: from genome to environment*, Academic Press, San Diego, 2011, pp. 1322–1331.
4 M. O. James, A. H. Altman, K. Morris, K. M. Kleinow and Z. Tong, *Drug Metab. Dispos.*, 1997, **25**, 346–354.
5 R. W. Kwong and S. Niyogi, *Comp. Biochem. Physiol., Part C: Toxicol. Pharmacol.*, 2009, **150**, 442–449.
6 K. Schirmer, *Toxicology*, 2006, **224**, 163–183.
7 A. Kawano, C. Haiduk, K. Schirmer, R. Hanner, L. E. J. Lee, B. Dixon and N. C. Bols, *Aquacult. Nutr.*, 2011, **17**, E241–E252.
8 M. Minghetti, C. Drieschner, N. Bramaz, H. Schug and K. Schirmer, *Cell Biol. Toxicol.*, 2017, **33**(6), 539–555.
9 M. Geppert, L. Sigg and K. Schirmer, *Environ. Sci.: Nano*, 2016, **3**, 388–395.
10 H. Schug, F. Begnaud, C. Debonneville, F. Berthaud, S. Gimeno and K. Schirmer, *Anal. Methods*, 2018, **10**, 4394–4403.
11 B. H. Kenzaoui, C. C. Bernasconi, H. Hofmann and L. Juillerat-Jeanneret, *Nanomedicine*, 2012, **7**, 39–53.
12 C. Jud, S. Ahmed, L. Muller, C. Kinnear, D. Vanhecke, Y. Umehara, S. Frey, M. Liley, S. Angeloni, A. Petri-Fink and B. Rothen-Rutishauser, *BioRes. Open Access*, 2015, **4**, 457–468.
13 C. Drieschner, M. Minghetti, S. Wu, P. Renaud and K. Schirmer, *ACS Appl. Mater. Interfaces*, 2017, **9**, 9496–9505.
14 C. Drieschner, N. T. K. Vo, H. Schug, M. Burkard, N. C. Bols, P. Renaud and K. Schirmer, *Cytotechnology*, 2019, **71**(197), 1–14.
15 H. J. Kim, D. Huh, G. Hamilton and D. E. Ingber, *Lab Chip*, 2012, **12**, 2165–2174.
16 P. Shah, J. V. Fritz, E. Glaab, M. S. Desai, K. Greenhalgh, A. Frachet, M. Niegowska, M. Estes, C. Jäger and C. Seguin-Devaux, *Nat. Commun.*, 2016, **7**, 11535.
17 Q. Ramadan, H. Jafarpoorchekab, C. Huang, P. Silacci, S. Carrara, G. Koklu, J. Ghaye, J. Ramsden, C. Ruffert, G. Vergeres and M. A. Gijs, *Lab Chip*, 2013, **13**, 196–203.
18 S. Kuiper, C. Van Rijn, W. Nijdam and M. C. Elwenspoek, *J. Membr. Sci.*, 1998, **150**, 1–8.
19 B. Srinivasan, A. R. Kolli, M. B. Esch, H. E. Abaci, M. L. Shuler and J. J. Hickman, *J. Lab. Autom.*, 2015, **20**, 107–126.
20 L. Griep, F. Wolbers, B. De Wagenaar, P. M. ter Braak, B. Weksler, I. A. Romero, P. Couraud, I. Vermes, A. D. van der Meer and A. van den Berg, *Biomed. Microdevices*, 2013, **15**, 145–150.
21 R. Kalluri, *Nat. Rev. Cancer*, 2003, **3**, 422–433.
22 B. Halamoda Kenzaoui, S. Angeloni, T. Overstolz, P. Niedermann, C. Chapuis Bernasconi, M. Liley and L. Juillerat-Jeanneret, *ACS Appl. Mater. Interfaces*, 2013, **5**, 3581–3586.
23 J. H. Sung and M. L. Shuler, *Biomed. Microdevices*, 2009, **11**, 731–738.
24 W. Zheng, Z. Wang, W. Zhang and X. Jiang, *Lab Chip*, 2010, **10**, 2906–2910.
25 M. Morigi, C. Zoja, M. Figliuzzi, M. Foppolo, G. Micheletti, M. Bontempelli, M. Saronni, G. Remuzzi and A. Remuzzi, *Blood*, 1995, **85**, 1696–1703.
26 J. Rogal, C. Probst and P. Loskill, *Future Sci. OA*, 2017, **3**, FSO180.
27 C. A. Schnaitman, *J. Bacteriol.*, 1971, **108**, 545–552.
28 V. R. Dayeh, S. L. Chow, K. Schirmer, D. H. Lynn and N. C. Bols, *Ecotoxicol. Environ. Saf.*, 2004, **57**, 375–382.
29 M. W. van der Helm, M. Odijk, J. P. Frimat, A. D. van der Meer, J. C. T. Eijkel, A. van den Berg and L. I. Segerink, *Biosens. Bioelectron.*, 2016, **85**, 924–929.
30 O. Y. Henry, R. Villenave, M. J. Cronce, W. D. Leineweber, M. A. Benz and D. E. Ingber, *Lab Chip*, 2017, **17**, 2264–2271.
31 M. W. van der Helm, O. Y. F. Henry, A. Bein, T. Hamkins-Indik, M. J. Cronce, W. D. Leineweber, M. Odijk, A. D. van der Meer, J. C. T. Eijkel, D. E. Ingber, A. van den Berg and L. I. Segerink, *Lab Chip*, 2019, **19**, 452–463.
32 K. Sundell, F. Jutfelt, T. Agustsson, R. E. Olsen, E. Sandblom, T. Hansen and B. T. Bjornsson, *Aquaculture*, 2003, **222**, 265–285.
33 A. Puliafito, L. Hufnagel, P. Neveu, S. Streichan, A. Sigal, D. K. Fygenson and B. I. Shraiman, *Proc. Natl. Acad. Sci. U. S. A.*, 2012, **109**, 739–744.
34 A. D. van der Meer and A. van den Berg, *Integr. Biol.*, 2012, **4**, 461–470.
35 T. Ostaszewska, K. Dabrowski, M. E. Palacios, M. Olejniczak and M. Wieczorek, *Aquaculture*, 2005, **245**, 273–286.
36 B. Press and D. Di Grandi, *Curr. Drug Metab.*, 2008, **9**, 893–900.
37 J. M. Sorrell and A. I. Caplan, *Int. Rev. Cell Mol. Biol.*, 2009, **276**, 161–214.

